ZrB_2 Nanosheets; Synthesis, Characterization, and Application

By

Sidra Tul Muntha

School of Chemical and Materials Engineering

National University of Sciences and Technology

2021

ZrB_2 Nanosheets; Synthesis, characterization and applications

Name: Sidra Tul Muntha

Reg. No: NUST 2018 NSE-06-00000274222

This thesis is submitted as partial fulfillment of the requirements for the degree of

MS in (Nano Science and Engineering)

Supervisor Name: Dr. Sofia Javed

School of Chemical and Materials Engineering (SCME)

National University of Sciences and Technology (NUST)

H-12 Islamabad, Pakistan

September 2021

Dedication

“I dedicate this thesis to my loving and supportive family”

Acknowledgments

All adoration to Allah Almighty who is the maker, maintainer, and the Regulator of the world. He is the One, who gives and enables to us to think, use our aptitude in information in accomplishing noteworthy answers for humankind in each field. Along these lines, I express my most prominent on account of Almighty Allah the all-inclusive and the engineer of the world, who has talented us the mind and instable nature development of information and body to accomplish our work as this task report. As Allah Almighty says in Quran:

"Read! In the name of your lord" (Alaq; 1st revealed ayah)

This Quranic verse sums up the entire importance of education in the lives of humans. I like to express my gratefulness to my very nice and respected supervisors **Dr. Sofia Javed**, my GEC Members **Dr.Zeeshan Ali, Dr. Iftikhar Gul**, **Dr. Rahim Jan** and **Dr. Aftab Akram** for their clear and patient guidance that directed me to fulfil my project and this thesis. Their cool and calm behaviour motivated me to do my best. Their valuable suggestions and feedback contributed greatly to this thesis. Also, I am very grateful to all my teachers who helped me and motivated me to do the best. I might likewise want to thank **my parents, family members, and companions** for their assistance, petitions, and their significant ideas.

I am thankful to all the faculty members to build my basis of Nano Science and Engineering. I want to thank **Mr. Akbar Ali, Mr. Usman Ali, Mr. Arman Liaqat, Ms. Saira Qayyum, Ms. Amr Min Allah, Ms. Kanza Iqbal, Ms. Zeenia Arzo, Ms. Maham Iqra and Ms. Amna** for their continuous support and motivation which helped me at various stages during my Masters.

I acknowledge the support provided by the Materials Engineering Department of SCME for providing me a platform to perform my experiments and using my skills in research work. I feel honoured to thank all the lab engineers, especially those who assisted me in all the possible manners.

I acknowledge the financial aid and technical assistance provided by our department, SCME, during my research experience and made this project work memorable forever. Last, but not the least, I want to thank my family for their prayers, support, and confidence in me without which I would not have been able to reach my full potential.

-Sidra Tul Muntha

Abstract

Among numerous super high temperature ceramics, Zirconium diboride (ZrB_2) has drawn in increasingly more consideration due to its unique combination of properties. As it has high melting point, high strength, high thermal and electrical conductivity, chemical inertness, and low density. Two-dimensional, zirconium diboride (ZrB_2) nanosheets are prepared through liquid phase exfoliation and the prepared samples are characterized through Scanning Electron Microscope (SEM), X-Ray Diffraction (XRD), UV-Vis spectroscopy, and Atomic Force Microscopy to determine morphology, phase analysis, optical properties, and dimensional aspects of nanosheets, respectively. The photocatalytic performance of ZrB_2 nanosheets were studied in comparison to TiO_2 nanoparticles. Commercial TiO_2 nanoparticles and exfoliated nanosheets are used to prepare ZrB_2 /TiO_2 nanocomposites with different weight compositions 0.5%, 1% and 2% (ZrB_2 nanosheets) to evaluate photocatalytic degradation of Rhodamine B. The photocatalytic behaviour studied under the UV light for photo degradation of Rhodamine B. From the photocatalytic results, it is inferred that 1% nanocomposite shows the best performance with about 85% degradation in just 60 minutes.

Table of Contents

List of Figures

List of Tables

List of abbreviations

2D……... Two Dimensional Materials

TMDs……. Transition Metal Diborides

MDs…….. Metal Diborides

UHTCs…… Ultra-High-Temperature Ceramics

ZrB_2 ……. Zirconium Diboride

TiO_2 ……. Titanium dioxide

NMP…… N-methyl-2-pyrrolidone

XRD……. X-Ray Diffraction

SEM……. Scanning Electron Microscopy

UV-Vis. …… Ultraviolet and Visible spectroscopy

BET…….. Brunauer Emmett Teller

AFM……. Atomic Force Microscopy

Chapter 01

Introduction

Nanotechnology is a promising field, it promises vital improvements of manufacturing techniques and advanced materials. It has applications nearly in every field of research. Nanotechnology has so much potential in research and development to address major problems [1]. The world is facing severe energy crisis. The need of the hour is to shift towards sustainable and green energy products [2]. Due to increased human population and growth in energy consumption the world's energy resources are depleting day by day. The dependence on fossil fuels like coal gas and natural oil is exceeding with an alarming rate. Due to this, fossil fuels are draining excessively. Also, the burning of these materials produces gases like CO_2 which are not only causing pollution in environment but is also a hazard for life on Earth due to global warming and greenhouse effect. Also, environmental and water pollution has become so fatal for human life. This pollution is becoming detrimental to human health [3]. Heavy metals and organic dyes are among the list of materials which pollute environment and cause serious health issues. Degradation of these water pollutants by employing light-absorbing materials under the solar spectrum is a highly efficient, and economical approach for the treatment of wastewater. Photocatalysis provides an easy way to remove the toxic organic dyes present in wastewater using solar radiation. [4][5]

1.1 Two Dimensional Materials

Two-dimensional (2D) objects are defined as layered objects that contain one (or a few) atomic monolayers. Previous to the separation of graphene, a single layer of graphite, in 2004 [6] 2D materials were considered for a long time as a class of purely academic materials that could not exist in a freestanding, atomically thin form. For example, Mermin suggested that objects in a two-dimensional form could remain virtually unstable, as a result in thermal fluctuations that prevent long-distance alignment with finite temperatures. Within this context, the first demonstration of a stable, free 2D object, Graphene, was a monumental discovery. Since the discovery of graphene, many other 2D materials have been discovered and

studied. Extensive research has been done to study physical, chemical, and electrical properties of these materials. [7]

Graphene is semi-metallic, other 2D materials have been found to be insulating (e.g. hexagonal boron nitride, h-BN), or semiconducting (e.g. molybdenum disulfide, MoS_2), or metallic (e.g. tungsten ditelluride, WTe_2), or superconducting (e.g. niobium diselenide, $NbSe_2$). Research efforts worldwide in 2D materials have been wide ranging, including topics such as (i) studying basic properties such as electron mobility, (ii) exploring novel quantum phenomena such as anomalous quantum Hall effect, (iii) isolating single or few layers from the bulk through mechanical exfoliation for researching their physics, (iv) synthesizing the 2D material directly on a desired substrate via various growth methods, for intended device application., (Figure 1.1), offers a wealth of possibilities, leading to new physics and interesting phenomena, with potential device applications.

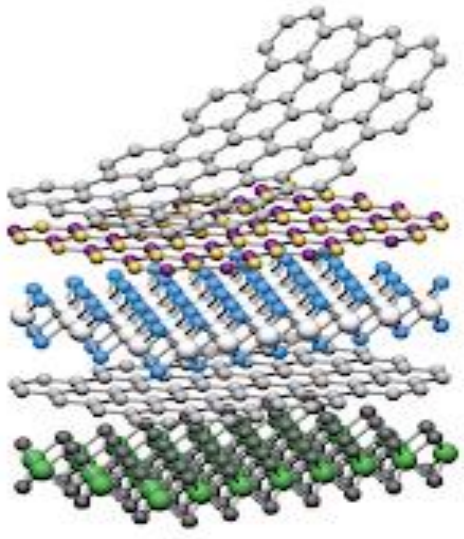

Figure 1.1 van der Waals heterostructures [61]

1.2 Transition Metal Diborides (TMDs)

TMDs are a family of materials of type MB_2, where M is a transition metal element (Mo, W, Zr, Nb, etc.) and B is Boron atom. [8] MB_2 are a class of layered materials that contain vertically stacked hexagonal boron sheets of graphene-like structure, with metal atoms sandwiched between the sheets as given in Figure 1.2. Every metal

atom is surrounded by 12 equidistant boron atoms which are present in the planes above and below the metal layer, and 6 metal atoms in the same plane. [9]

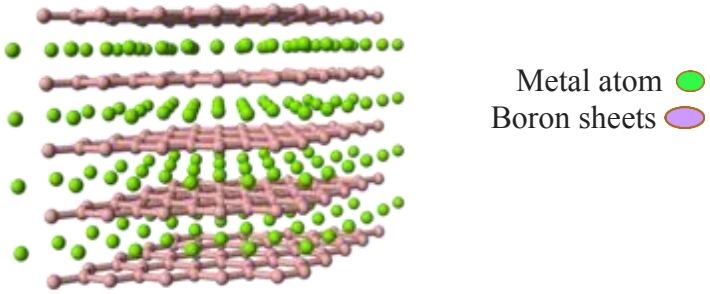

Figure 1.2 Metal diborides structure [62]

TMBs are a main class of ultra-high temperature ceramics (UHTC). They are encouraging for many applications due to their thermomechanical and chemical properties, high melting temperature up to~ 3300 ^{o} C and excellent strengths at high temperature as shown in the Table 1. The diborides of group IV-XII are known as transition metals, which are usually hard and dense, and also good conductors of heat and electricity. [10, 11]

Table 1 Physical properties of some borides

Boride	**Density (10^3 kgm^{-3})**	**Melting point (^{o} K)**	**Electrical resistivity (10^{-8} Ωm)**	**Hardness, 1 N load**	**Crystal system and structural type**
TiB_2	4.52	3470	9-15	2600	Hexagonal, AlB_2 type
ZrB_2	6.09	3520	7-10	1830	Hexagonal, AlB_2 type
HfB_2	11.2	3650	10-12	2160	Hexagonal, AlB_2 type
VB_2	5.10	2670	16-38	2110	Hexagonal, AlB_2 type
NbB_2	7.21	3270	12-65	2130	Hexagonal, AlB_2 type

1.2.1. Bonding in Metal Diborides

The nature of bonding present between the alternating metal and boron layers is very different from previously discussed van der Waals solids, such as graphite.

In case of van der Waals solids, there are strong covalent bonds present between atoms in the individual layers, and these individual layers are held together by weak van der Waals forces. [12] The case of MB_2 is more complex as they possess mixed bonding characteristics. For diborides of main group elements, such as magnesium and aluminium, the nature of bonding between the metal-boron layers is predominantly ionic, which arises due to the electron transfer from metal to boron atoms. Within the boron layer, covalent bond is present, however, the atoms in the metal layer have negligible metallic bonding. In contrast, in transition metal diborides, such as hafnium and zirconium, the nature of bonding between the metal-boron layers is a mixture of covalent and ionic. Apart from the electron transfer from metal to boron layer, the partial interaction of d electrons of metals with p-electrons of boron imparts the covalent character to the metal boron bond leading to a more complex bonding environment. The atoms in the boron layer are covalently bonded, and the ones in the metal layers have bonds with both metallic and covalent characteristics [13]

1.2.2. Applications of Metal Diborides

MB_2 have attracted considerable attention over the years due to their remarkable physical and chemical properties such as hardness, thermal conductivity, and high melting temperatures. With every metal comes a different set of properties: MgB_2 is a well-known superconductor at 39 K; [14] TiB_2 has a very high melting temperature and shows electrical conductivity higher than the titanium metal itself; [15] ZrB_2 and HfB_2 are UHTCs [16] with applications in aerospace industry, such as building components of atmosphere re-entry vehicles; and ReB_2 and OsB_2, [17] which contain puckered boron sheets instead of planar sheets, are ultra-hard materials with Vickers hardness over 40 GPa, which is the limit for ultra-hard materials. [18]

1.3 Zirconium Diboride (ZrB_2)

TMBs are an exceptional class of UHTCs. Among these TM compounds, refractory borides such as ZrB_2, TiB_2, TaB_2, and HfB_2 appealing contender for different applications like cutting apparatuses, molten metal containments, and microelectronics. [14]

ZrB_2 is one of the super-high temperature ceramics that have earned the most consideration as potential competitor for leading edge materials because their oxidation resistance is superior to the other borides. [15] ZrB_2 shows an amazing combination of ceramic like strength (23 GPa or higher at room temperature) and elastic modulus (~ 500 GPa at room temperature) with metal like electrical (~ 10^7S m^{-1}) and thermal (>60 W m^{-1} K^{-1}) conductivities. [16] Many of the important physical, structural and thermodynamic properties are shown in Table 2.

Table 2 Physical, structural and thermodynamic properties

Properties	ZrB_2
Melting temperature (^{0}C)	**3245**
Crystal structure	**Hexagonal**
Theoretical density (g cm^{-3})	**6.1**
Hardness (GPa)	**23**
Thermal conductivity at 25 ℃ (W m^{-1} K^{-1})	**60**
Electrical conductivity (S m^{-1})	**$10.0*10^6$**
Coefficient of thermal expansion (K^{-1})	**$5.9*10^{-6}$**
Young's modulus (GPa)	**489**

1.4 Lattice structure of ZrB_2

The hexagonal AlB_2-type structure of ZrB_2 accumulates with P6/mmm space group (No. 191). One ZrB_2 formula unit is contained in the unit cell. Each Zr atom has six equidistant neighbours. In its plane, each B is surrounded by three B neighbours and six Zr atoms out of the plane. The crystal structures of ZrB2 are illustrated in Fig. 3.

Table 3 declared crystal structure, lattice parameters, and some other physical and chemical properties, together with assailable experimental and calculated data in contrast.

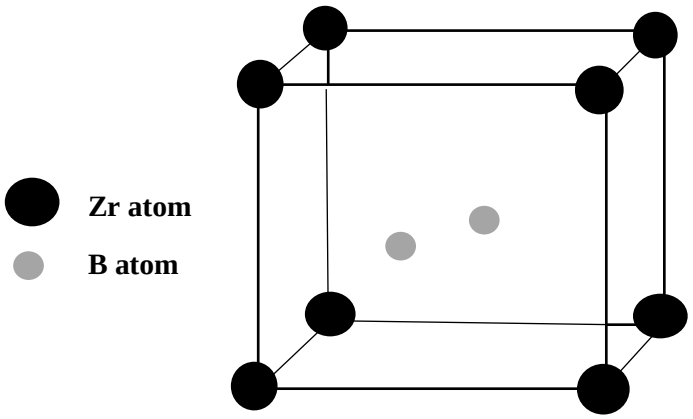

Figure 1.3 Crystal structure of ZrB_2 [63]

Table 3 Structure data of ZrB_2 and heat of formation

Structure data of ZrB_2 and heat of formation	**ZrB_2 Experimental**	**ZrB_2 Calculated**
Space group (No.) Crystal system	P6/mmm (191) Hexagonal	P6/mmm (191) Hexagonal
Lattice constants a, c (Å)	a = 3.169, c = 3.530	a = 3.197, c = 3.561
Volume ($Å^3$)	30.701	31.520
-△H (kJ/mol)	322.59	296.81

1.5 Synthesis routes:

In this project top down approaches are used for the synthesis of Zirconium diboride nanosheets which are discussed below:

1.6 Bottom-up approaches:

Also, there are many ways to develop 2D materials via bottom-up approaches like:

1. Wet chemical synthesis

2. Chemical vapour deposition

1.6.1 Wet chemical synthesis:

By this method, the objective materials are arranged utilizing forerunners, and synthetic responses occur in the arrangement. Certain surfactants are added to poise the size, shape, and the morphology of target materials to be delivered [35]. One broadly applied wet-synthetic strategies for the nanomaterials include template synthesis, hydro or solvo thermal synthesis, self-assembly of the nanocrystals, and the soft colloidal production [36].

1.6.2 Merits:

• All 2D materials sheets, metals, transition metal-oxides and the metal chalcogenides can be synthesized by this method.

• High return of 2D nanomaterials for minimal price can be accomplished.

• Control on morphology of nanomaterials is more in wet compound strategies

1.6.3 Demerits:

• Difficult to achieve single layer of 2D Nano sheets

1.7 Top down Approach

1.7.1. Mechanical exfoliation:

In this way, the layers are isolated utilizing explicit powers [37]. Graphene was combined utilizing this technique utilizing a great deal of graphite utilizing the "scotch tape strategy" [38]. Along these lines, great mono sheets can likewise be fabricated. This strategy is mainstream as it produces inside sheets and an enormous space of exploration is presently centred around it.

1.7.2. Merits:

- Usually, in this way, clean quality sheets are obtained.

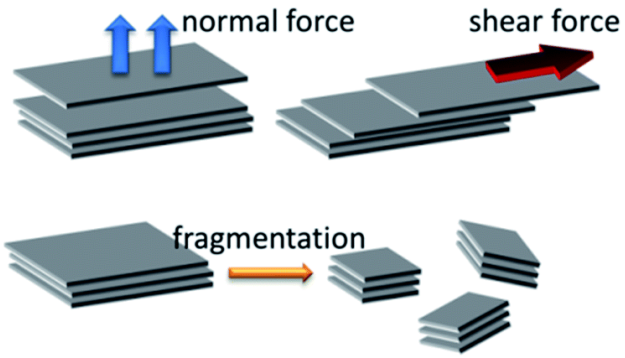

Figure 1.4 Mechanical Exfoliation of 2D materials [64]

1.7.3. Demerits:

- Low yields are achieved in this process.
- And in this way, there is a lack of chaos.
- This method does not apply to production on a large local scale.
- Sheet size and thickness control are problematic.

1.7.4. Liquid phase exfoliation:

In this way, solvents are used to separate the computer layers. These solvents used for their higher energy are compatible with those of crystalline glass [39]. Sonication produces single-layer Nano sheets and multilayers remain stable where there is a solvent / surfactant suitable for the reaction or distribution component [40]. Other surfactants can also be added to it to obtain well-defined properties. Sonication assisted oil extraction is now widely used in the preparation of mono-, few-loaded structures from bulk. In sonication sound forces are used which lead to shear forces. Cavitation bubbles are produced which, in the event of a collapse, burst layers [41]. Solvent selection is an important choice, that is, it should speed up the separation process. It should deliver a very stable spread with high density of 2D extruded sheets. Sometimes a combination of non-liquid chemicals can also be used to produce products effectively. In non-liquid chemicals, N-methyl-2-pyrrolidone (NMP) is widely used. NMP has a strength of more than ~ 40mJm-2 which is similar to the higher strength of multi-stranded material [39]. In NMP, one can achieve a stable distribution of graphite up to 40mg / ml with a maximum strength of ~ 75mJm-

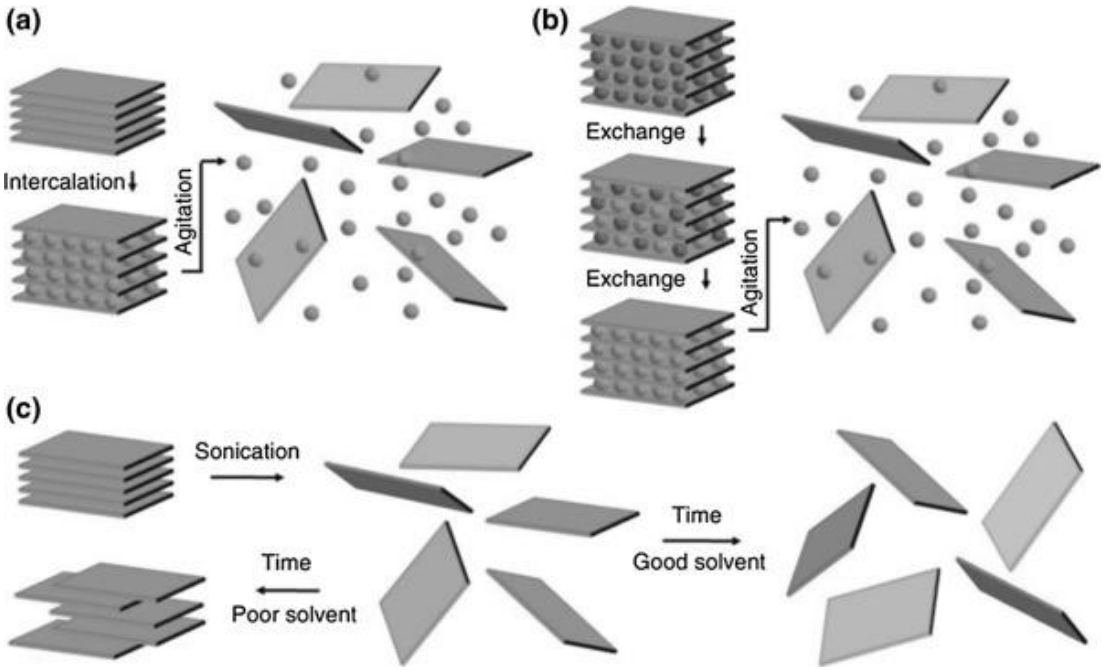

Figure1.5 Liquid phase exfoliation of 2D materials [65]

1.7.5 Merits:

- A great harvest is found in this process.
- This method is non-ventilated.
- Excludes chemical reactions.
- The highest quality crystal product is available.
- This method is simple and inexpensive.
- Spreading spreadsheets are available

1.7.6 Demerits:

- Solvent exfoliation contains residual chemicals present in it that can affect Nano sheet structures such as graphene. The solvent may change and become toxic as well.

1.8 Photo catalysis

The utilization of solar energy for initiating reactions is already been applied [28]. Many photo induced reactions have been developed and utilized since sunlight is most abundant in nature. A reaction that uses a photo catalyst (that itself remains unconsumed at the end of reaction), which is usually a semiconductor; to accelerate a

chemical reaction in the light is known as Photo catalysis. When the light is absorbed on the surface of the photo catalyst free holes (hvb) and free electrons (ecb) are created [29].

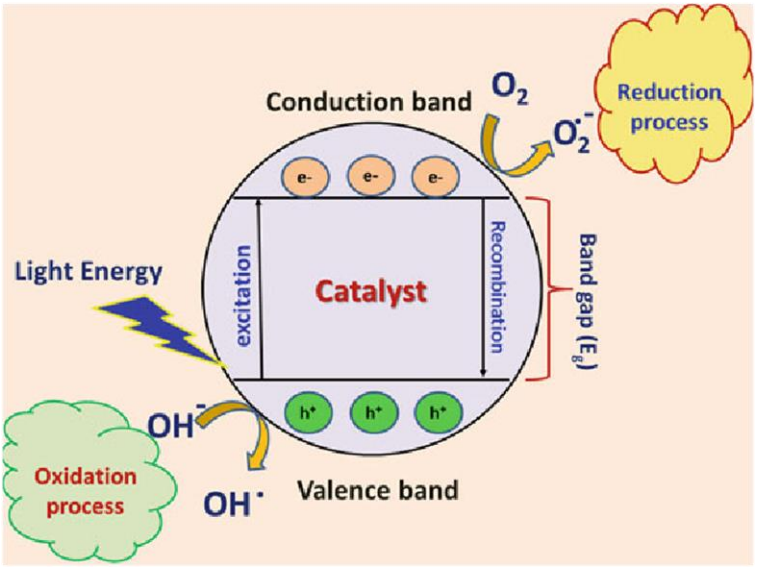

Fig.1.6 Mechanism of Photocatalysis [60]

Mostly the general catalytic reaction consists of an oxidation reaction from the free electron and a reduction reaction from the hole.

4hvb ++ $4H_2O$ O_2 + 4H+ (oxidation reaction)

O_2 + 4H+ + 4ecb - $2H_2O$ (reduction reaction)

Generation of a free electron and free hole is necessary for good oxidizing capabilities. In case of semiconductors, the band gap must be bridged. Sufficient amount of energy must be provided by the incident light so that the electron gets energized enough to move from valence band to the conduction band. The energy (E) brought by a photon is given by:

$$\boldsymbol{E = hc / \lambda}$$

1.8.1 Advantages of ZrB_2 in photo degradation:

➢ It is chemically, thermally and mechanically stable.

➢ It is inexpensive

➢ The formation of photo cyclized intermediate product is avoidable.

➢ No solid waste disposal problem occurs.

Chapter 2

Literature review

In the field of nanomaterials, two-dimensional nanomaterials show immense potential and applications due to their unique physicochemical properties. Due to the novel properties of metal diborides, they become encouraging for many applications. In the latter years, researchers are trying to exfoliate transition metal diborides, and ZrB_2 has been used in various mechanical applications. Continuous efforts of exfoliating layered materials have contributed new applications.

ZrB_2 is ultra-high temperature ceramic and novel due to its hardness, high melting temperature, and thermal conductivity it can be further applicable for EMI shielding, energy storage and aerospace applications. The potential of ZrB_2 has been investigated at micro level but there is a surge for nanomaterials with superior physical and chemical properties.

A. Yousaf et al. reported the synthesis of 2D nanosheets of metal diborides including AlB_2, CrB_2, HfB_2, NbB_2, MgB_2, TiB_2, TaB_2, and ZrB_2, via ultra-sonication-assisted exfoliation. Tip sonication and bath sonication methods were used for exfoliation and each metal diboride powder was mixed with a suitable organic solvent or aqueous surfactant solution to make dispersions. The lateral dimension of exfoliated sheets has a length up to micrometers and thickness down to 2-3 nm. The exfoliated metal diboride layers retained their chemical composition and hexagonal structure with a lateral dimension up to micrometers and thickness down to 2-3 nm. TEM results showed the size of flakes varying from 100 nm across to several microns across and morphologies like flat, planar sheets for Mg, Al, Ti, and Cr diborides and folded, crumpled for Zr, Nb, Hf, and Ta diborides. AFM results showed thicknesses varying between 3 to 18 nm and lateral dimensions from 150 nm to 4 μm across.[59]

Wang L. et al. reported the synthesis of ZrB_2 nanosheets by using zirconium dioxide, iodine and sodium borohydride via solid state route. ZrB_2 nanosheets were produced with the dimension of 500nm and thickness 20nm at 700^0 C in autoclave. [50]

An Y. et al. reported the effect of ZrB_2-SiC graphene ceramic composite by using commercial raw material through hot pressing method. Due to the effect of SiC

whisker and graphene nanosheets, flexural strength and fracture toughness are both improved. [48]

Table 4 Literature summary

Material	**Method**	**Properties**	**Application**	**Reference**
SiC, ZrB_2 , graphite	Plasma spray method	Ablation behaviour of SiC/ ZrB_2 coatings are controlled by the formation of ZrO_2 dense layer	Leading edges, re-entry missiles nozzles throat, propulsion systems	Torabi S. et al. [53]
Zirconium, silicon powder	Hot pressing method	In situ composite of ZrB_2 and SiC formed that were found in agglomerates with particle size ranges.	Synthesis reported	Zhang G. et al. [47]
$Zr(OPr)_4$ H_3BO_3 , $C_{12}H_{22}O_{11}$, and AcOH.	Sol gel method	different shapes of particles achieved	Synthesis reported	Zhang Y. et al. [49]
$NbSe_2$ powder, NMP as a solvent, TTIP, Glacial acetic acid, distilled water and HNO_3	Liquid phase exfoliation for Nano sheets and sol gel method for TiO_2 Nano particles	Improved photo degradation to 98%.	Photo catalysis	Khan, R .et al. [53]

MoS_2 powder, NMP as a solvent, TTIP, Glacial acetic acid, distilled water and HNO_3	Liquid phase exfoliation for Nano sheets and sol gel method for TiO_2 Nano particles	Reached constant rate reaction by 0.559 hr^{-1} by 2% addition of nanosheets.	Photo catalysis	Khan, R .et al. [52]
Commercially available ZrB_2 ,H_2, Ar and CH_4	Chemical Vapour Deposition	CNS/ZrB_2 particles improved the fracture toughness of ZrB_2 based composites	Synthesis reported	An Y.et al. [51]

ZrB_2 is ultra-high temperature ceramic and novel due to its hardness, high melting temperature, and thermal conductivity it can be further applicable for EMI shielding, energy storage and aerospace applications. The potential of ZrB_2 has been investigated at micro level but there is a surge for nanomaterials with superior physical and chemical properties. So, in this research project ZrB_2 nanosheets will be synthesized and its potential as a photocatalyst material will be investigated.

2.1 Aims and objectives

The aim of this study is to:

- Synthesize and characterize Zirconium diboride nanosheets.
- To investigate photocatalysis of ZrB_2/TiO_2 nanocomposites.

Chapter 3

Experimentation

3.1 Synthesis of ZrB_2 Nanosheets

ZrB_2 nanosheets are prepared through liquid phase exfoliation. 50 mg/ml solution of ZrB_2 is sonicated in 80mL NMP. Purpose of NMP used as a solvent for this method is as it has an ability to overcome the strong forces present between the ZrB_2 layers. ZrB_2 sheets are obtained by using probe sonicator for 6 hours with 80% amplitude. Then the exfoliated nanosheets are centrifuged at 1500, 1000 and 500 RPM for 60 mints respectively in a centrifuge machine. From centrifugation, compact and light weight nanosheets are separated and after that ZrB_2 nanosheets are filtrated over nylon membrane by the use of vacuum filtration. The nanosheets are then detached from the filter paper to characterize them.

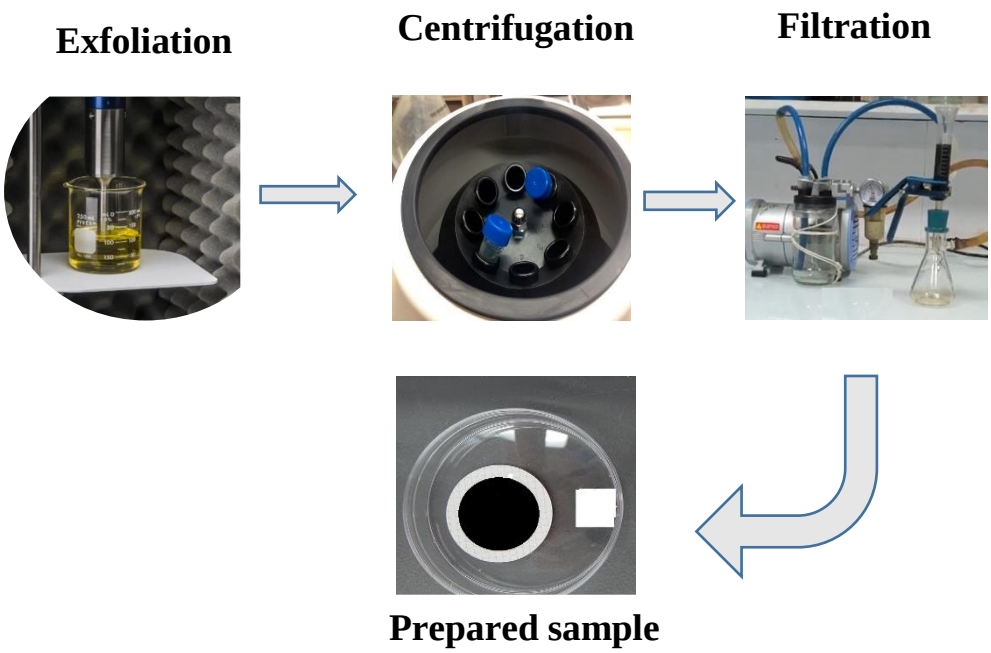

Fig.3.1 Synthesis Route for preparation ZrB2 nanosheets

3.2 Synthesis of Nanocomposites (ZrB_2 /TiO_2)

Commercial Titania is used to prepare ZrB_2 /TiO_2 nanocomposites. Separate mixtures of TiO_2 and ZrB_2 in 2-propanol (50mg/ml) were sonicated for 1 hour in probe sonicator for homogeneous dispersions. Both these dispersions are utilized to make composites with ZrB_2 weight 0.5%, 1% and 2% through the bath sonicator for 2 hours. Afterwards, the solvent was dried away in oven at 80 °C and the composite samples were ready for further characterization and application.

3.3 Characterization of Samples

The analysis of the synthesized nanosheets and nanocomposite was performed by the following characterization techniques:

3.3.1 X-Ray Diffraction (XRD)

XRD was performed using powder samples of nanosheets and nanocomposite, without involving any sample preparation step.

3.3.2 Scanning Electron Microscopy (SEM)

For SEM analysis powder samples were sonicated in ethanol for 2 hours and then drop- cast on clean glass slides followed by drying of samples at 80 °C.

3.3.3 Atomic Force Microscopy (AFM)

AFM analysis also required sonication of powder samples in ethanol for 2 hours then drop-casting on clean silica slides and subsequent drying at 80 °C for evaporation of ethanol.

3.3.4 UV Visible Spectroscopy

UV analysis required homogenous dispersion of powder samples. The powder samples were sonicated for 3 hours in NMP (N-Methyl-2-pyrrolidone). 2 ml of each

dispersion was used for UV analysis. The ZrB_2/TiO_2 nanocomposites were further employed for photocatalytic degradation of Rhodamine B dye.

3.3.5 Brunauer Emmett Teller (BET)

Surface area and porosity is the vital property of a material which can be determined by BET analysis technique. For sample preparation 200 mg of sample is purified by degassing to remove the extra atmospheric contaminants like water vapors and air at 150 ^{o}C. Then the sample analysis was performed using Gemini® VII 2390 instrument. Operating conditions were degassing of the sample at $300°C$ for 3 hrs. and analysis were performed at 0.05 to 0.3 p/p0 range.

3.4 Photocatalysis of Rhodamine B

The photocatalytic degradation efficiency of the prepared ZrB_2 /TiO_2 nanocomposites was tested by degradation of an organic dye rhodamine B. To prepare dye solution, 1 mg of Rhodamine B was taken in 1 L of deionized water and prepared a homogeneous mixture. Each ZrB_2 /TiO_2 nanocomposites sample was added in of dye solution (1mg/1ml) to study their effect on dye photodegradation. The readings of degradation are taken after 15 mins intervals.

Chapter 4

Results and discussion

Exfoliated ZrB_2 nanosheets and prepared nanocomposites (ZrB_2/TiO_2) are characterized by X-ray diffraction (XRD), scanning electron microscope (SEM), UV-Vis spectroscopy, atomic force microscopy (AFM) to study the phase, morphology, optical properties and dimensional aspects of ZrB_2 nanosheets and the composites respectively.

4.1 Characterization of ZrB_2 nanosheets

XRD is done to characterize the phase of ZrB_2 nanosheets. Figure 4.1 a) represents the XRD pattern of bulk ZrB_2 and exfoliated nanosheets at 500 RPM, 1000 RPM, and 1500 RPM. The hexagonal aspect of bulk ZrB_2 is characterized by the peaks at 25.2^o, 32.6^o ,41.6^o ,51.7^o ,58.1^o ,62.5^o ,64.4^o ,68.2^o ,74.0^o and 81.5^o which corresponds to the (001), (100), (101), (002), (110), (102), (111), (200), (201) and (112) Planes, respectively, conformable with the reported value of ZrB_2 (JCPDS cards, No. 65-3389).

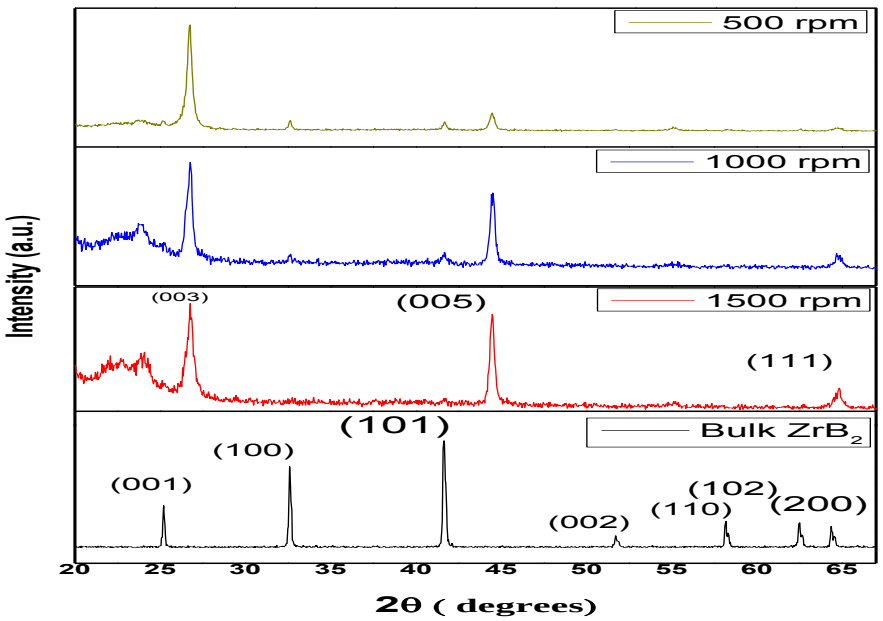

Figure 4.1 XRD spectra of Bulk ZrB_2 and exfoliated ZrB_2 nanosheets at 500 RPM, 1000 RPM and 1500 RPM

Exfoliated Nano sheets are shifted at some angles as given in the figure 4.1 a), Broadness of peaks in 1000 and 1500 RPM separated ZrB_2 Nano sheets in comparison to bulk as shown in figure 4.1 a), as the peaks observed at 32.6°, 41.6°, 64.4° and 81.5° corresponds to (100), (101), (111) and (112) planes respectively, conforms that there will be a part of bulk is also present along Nano sheets in 500 RPM.

UV-Vis Spectroscopy is carried out to characterize the optical properties of ZrB_2 nanosheets. Figure 4.2(a) shows the UV-Vis spectrum of ZrB_2 nanosheets at 500, 1000, 1500 RPM and bulk ZrB_2, showing the UV light absorption in the ZrB_2 nanosheets. A solid absorption band shows at around 270 nm owing valence band to conduction band at the plane of ZrB_2 nanosheets [55].

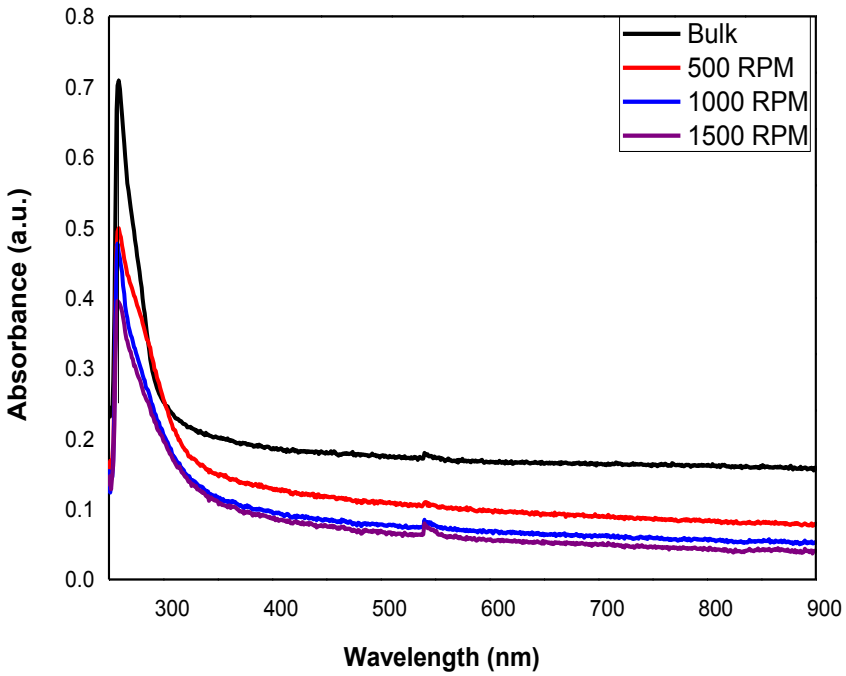

Fig. 4.2 UV-Vis spectra of Bulk ZrB_2 and ZrB_2 Nano sheets at 500 RPM, 1000 RPM and 1500 RPM

SEM is done to characterize the morphology of ZrB_2 Nano sheets. Figure 4.3(a, b, c) show the morphology of thin Nano sheets as a result of liquid phase exfoliation at 500 RPM, 1000 RPM, 1500 RPM respectively, in comparison to the bulk ZrB_2 (figure 4.3 d). Average Lateral dimension obtained at 500 RPM is 637.435nm, 590.925 nm at 1000 RPM and 569.23 nm at 1500 RPM.

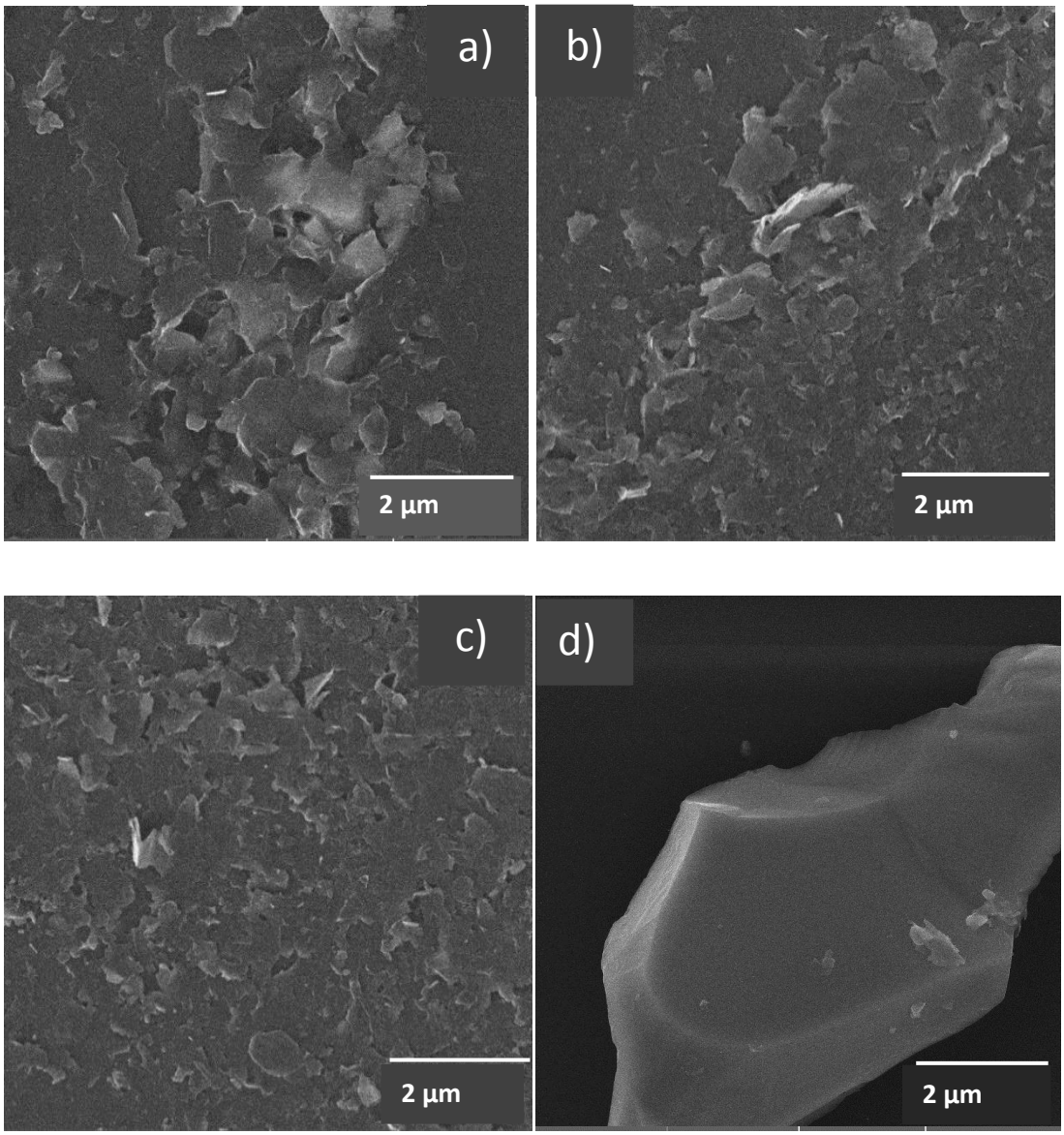

Fig. 4.3 SEM images of (a) exfoliated ZrB_2 Nanosheets at 500 RPM (b) at 1000 RPM (c) at 1500 RPM (d) Bulk ZrB_2

AFM is done to characterize the dimensional aspect of ZrB_2 Nano sheets prepared via liquid phase exfoliation. Thickness of Nano sheets can be estimated from the obtained results. Average thickness as measured from AFM is 8.37nm at 1500 RPM, 11.1nm at 1000 RPM while 13.1nm at 500 RPM. Figure 4.4 a) show the 13.5nm thickness of Nano sheets at 500 RPM, figure 4.4 b) show 11.1nm thickness at 1000 RPM and figure 4.4 c) show 9.77nm thickness at 1500 RPM. [52]

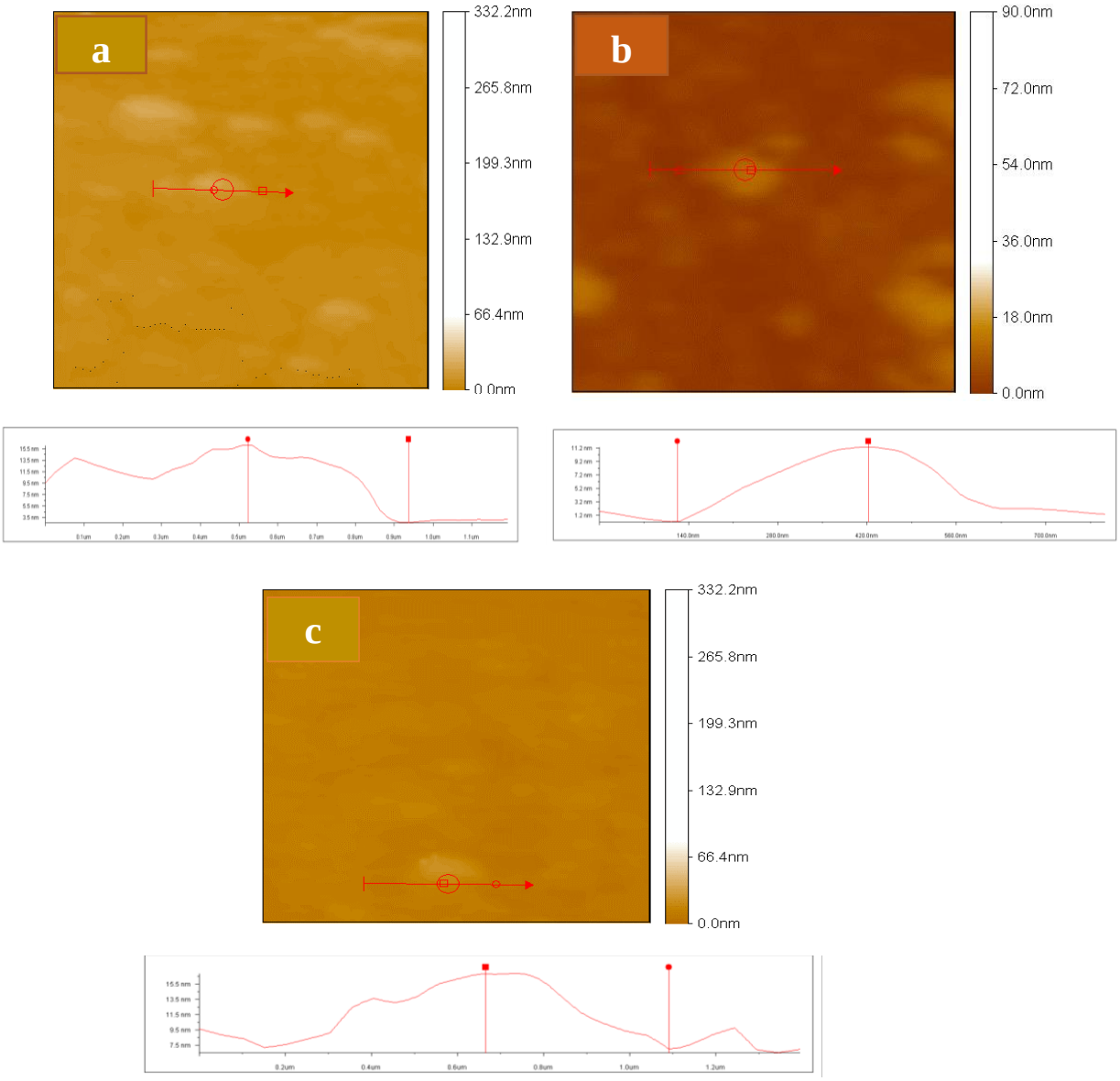

Fig. 4.4 AFM of exfoliated ZrB_2 Nano sheets with height of flakes a) 500 RPM b) 1000 RPM c) 1500 RPM

4.2 Characterization of ZrB_2 /TiO_2 nanocomposites

In figure 4.5 XRD of composites (ZrB_2 /TiO_2) and pure TiO_2 is shown. Titania is characterized by the peaks at 25.2 °, 38.5 °, 47.98 °, 53.76 °, 54.99 °, 62.57 °, 68.59 ° and 70.19 °, approves the formation of anatase TiO_2 Nano particles and corresponds to the (101), (112), (200), (105), (211), (204), (116) and (220) planes respectively[56]. While the peak at 27.3 corresponds to the (003) plane, confirms the presence of Nano sheets. With increase in content of ZrB_2 Nano sheets in Nano

composites from 0.5% to 2%, the peak becomes apparent. So figure 4.5 confirms the formation of composites. [53]

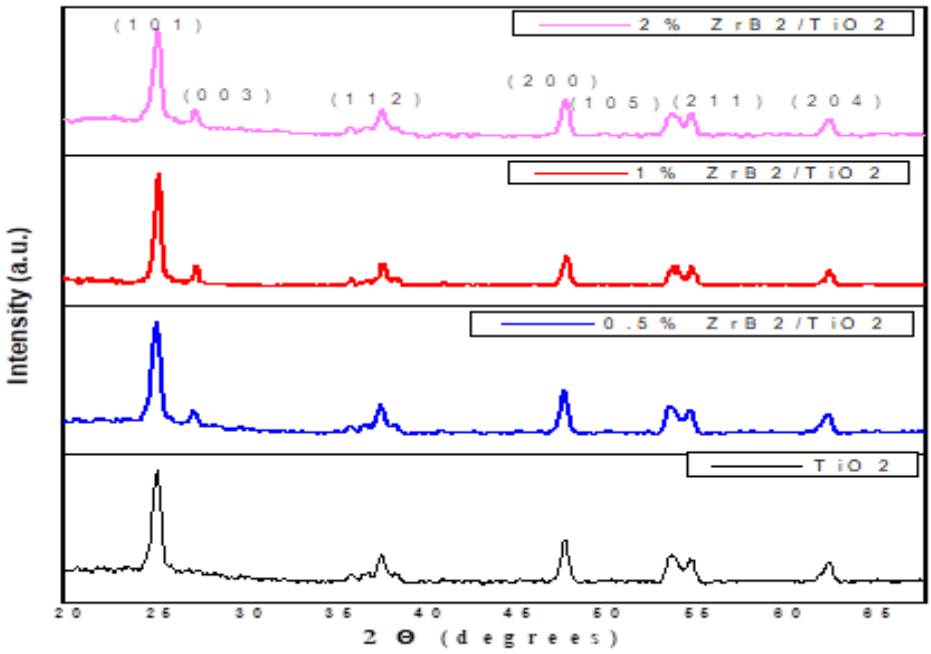

Fig.4.5 XRD spectra of Nanocomposites at different weight ratios

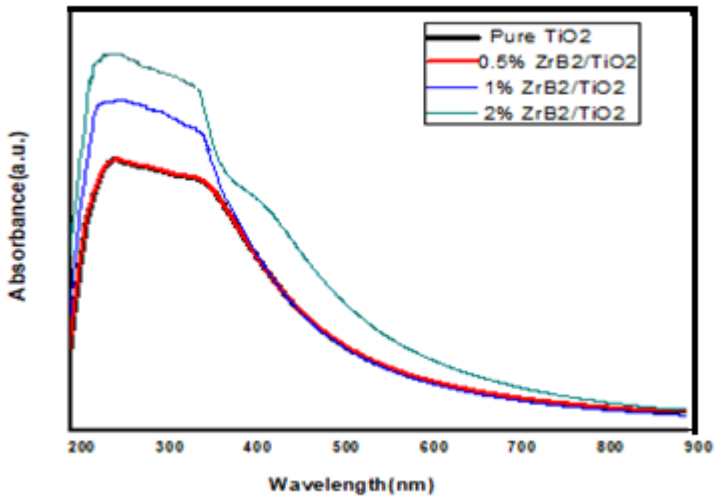

Fig. 4.6 UV-Vis spectra of Nanocomposites at different weight ratios.

In figure 4.6 it can be seen that 0.5% composite spectra is somewhat similar to that of bulk one which means that particles are fully loaded on Nano sheets which is confirmed by the SEM results. But in 1% and 2% composite absorption increases in

UV region. From the spectra, it can be clearly seen that by increasing the content of ZrB2 Nano sheets in composites UV light absorption increases [53]

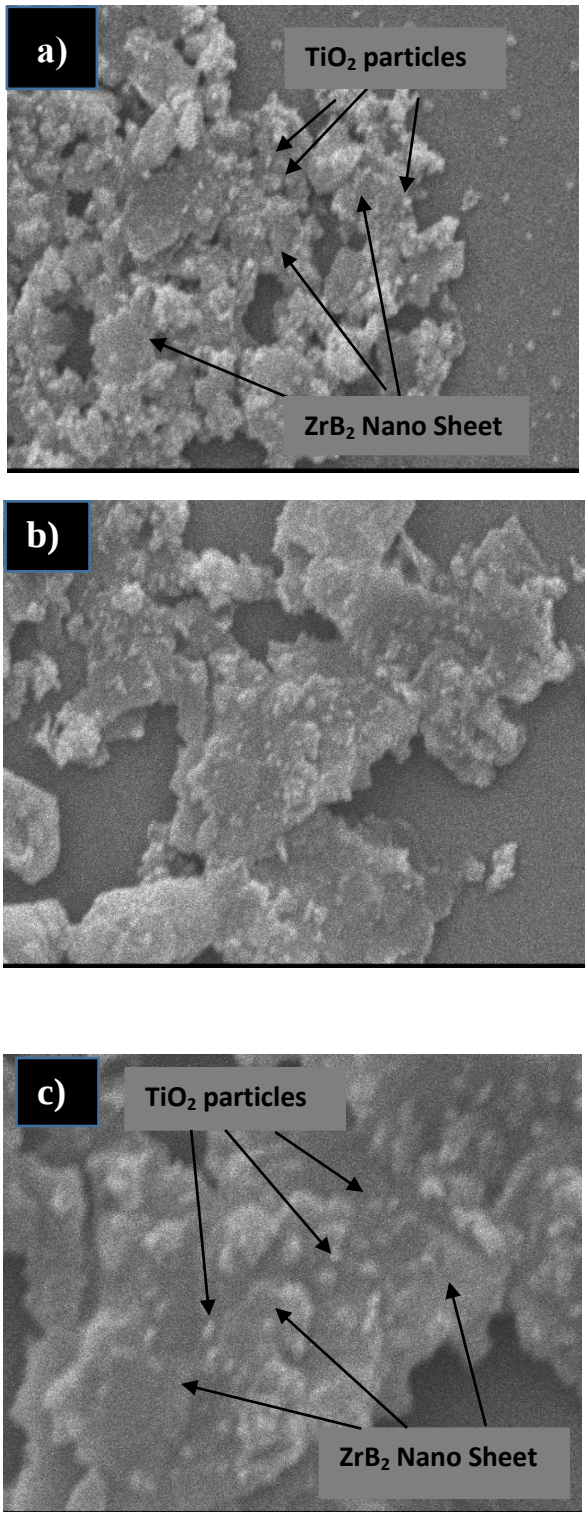

Fig. 4.7(a,b,c) SEM images of nanocomposites

While figure 4.7shows the formation of composites. TiO_2 nanoparticles ranges in 16nm-50nm with a uniform size distribution [59]. Attachment of TiO_2 nanoparticles over the surface of Nano sheets can be clearly seen.

4.3 BET Surface Area Analysis

BET used to decide the surface space of the pre-arranged composites. It has been seen that with expansion in substance of ZrB_2 Nano sheets inside TiO_2 Nano particles, the surface region increments up to 1 weight % i.e. till 1% ZrB_2 /TiO_2. Further expansion of ZrB_2 results in the surface area reduction for 2% ZrB_2 /TiO_2 as shown in Table 5.

The diminished surface region can be because of the less ideal circulation of ZrB_2 sheets as displayed in SEM results. The Nano sheets are aggregated in 2% ZrB_2 /TiO_2, bringing about decrease of surface region. [53]

Table 5 BET of prepared samples to figure the surface area

Serial no.	Samples	Surface area (m^2 /g)
1	Pure TiO_2 nanoparticles	36.66
2	0.5% ZrB_2 /TiO_2	42.55
3	1% ZrB_2 /TiO_2	55.92
4	2% ZrB_2 /TiO_2	50.81

4.4 Photo degradation Analysis

To prepare dye solution, 1 mg of Rhodamine B was taken in 1 L of deionized water. Prepared samples (0.5% ZrB_2 /TiO_2, 1% ZrB_2 /TiO_2, 2% ZrB_2 /TiO_2) are added in 50 ml of dye solution to study their effect on dye photo degradation. The mixture is irradiated with UV light in the UV reactor. The progress of photo degradation is studied using Beer Lambert law (A= εcl) with UV/Vis spectra. The readings of

degradation are taken after 15 minutes intervals. It is seen that, 1% ZrB_2 /TiO_2 is more efficient for photo degradation than 2% ZrB_2 /TiO_2. The (reaction rate) efficiency of dye degradation is calculated by:

Degradation efficiency= $(C_0-C_t)/C_0$ *100%

Where C_0 and C_t is the initial concentration and concentration at time t of dye.

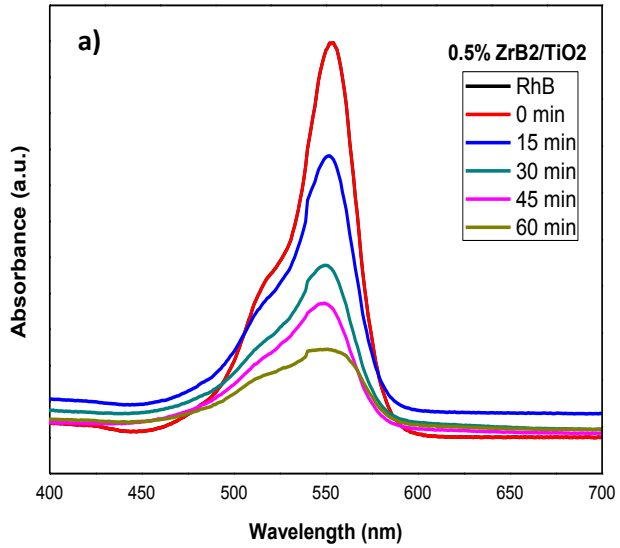

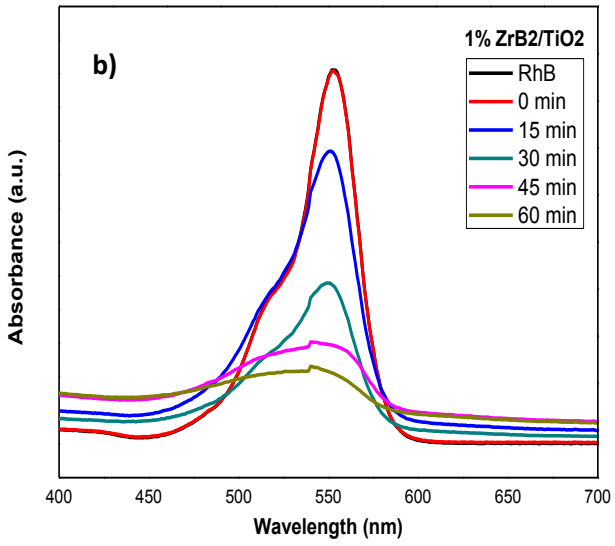

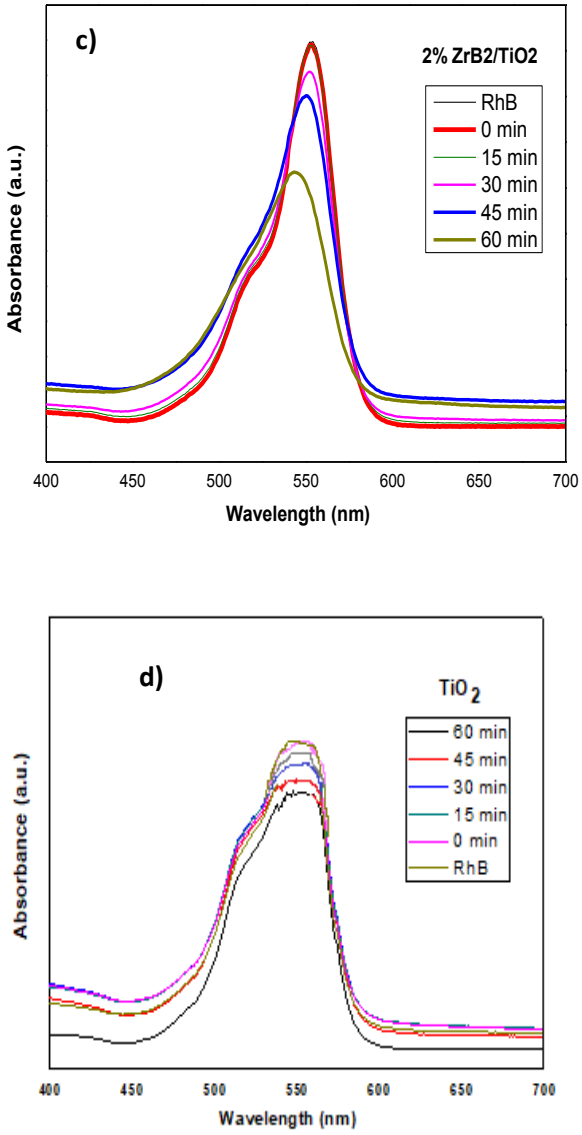

Fig 4.8 (a,b,c) UV-Vis spectra of RhB dye degradation caused by prepared composites (d) Pure TiO_2

Figure 4.8 shows the improvement of photo degradation process under UV light spectrum obtained after every 15 min during the reaction. It can be clearly seen in the figure that the absorbance by RhB decrease with time. Complete degradation of RhB dye by 1% ZrB_2 /TiO_2 is observed in 60 min. The efficiency of 2% ZrB_2 /TiO_2 decreases as compared to 1% ZrB_2 /TiO_2 due to contributing lower surface area as compared to 1% ZrB_2 /TiO_2. Because of the aggregation of ZrB_2 Nano sheets in 2% ZrB_2 /TiO_2, the photocatalytic activity under UV light is decreased. [52,53]

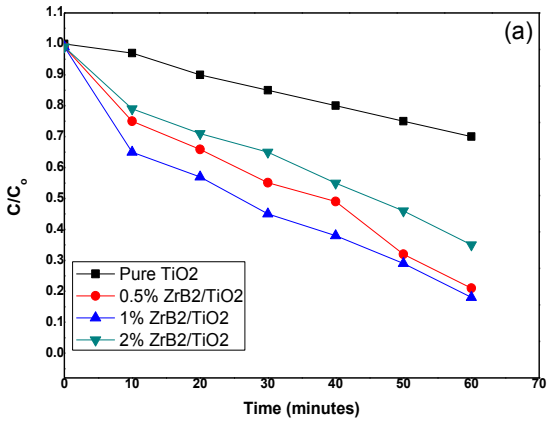

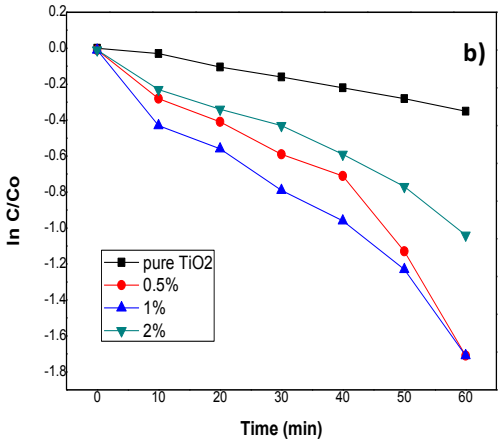

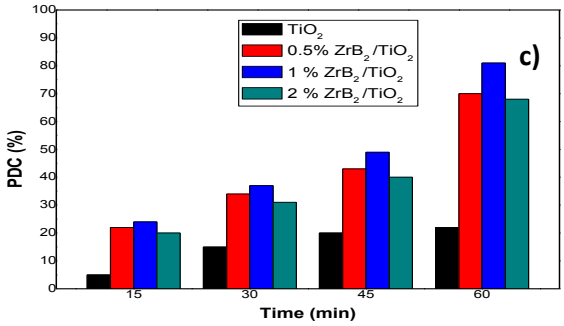

Figure 4.9 (a) C/Co plot of TiO_2 Nano particles and prepared composites to represent the photo degradation (b) Log plots of degradation efficiency to determine the rate constant (c) Percentage degradation of Rhodamine B as a function of increasing time

Figure 4.9 (a) shows photo degradation of Rhodamine B as a function of C_t/C_0 and fig. 4.9 (b) shows Log plots of degradation efficiency the rate constant determination. The photocatalytic degradation efficiency (PCD) was calculated using the Eq.1.

% Degradation = (1- C_t/C_0) x 100 ……..(1)

Based on above analysis, the plausible photo-response mechanism is proposed. As TiO_2 is sensitive to UV light, under illumination electron-hole pairs were generated. In figure 4.6, schematic represents the photo degradation of prepared ZrB_2 /TiO_2 nano composites. When light source is incident on TiO_2 nano particles, electron from the valence band jumps into the conduction band, forming a hole in the valance band of TiO_2 nanoparticles and then further transfer to the conduction band of ZrB_2 nano sheets. There is a possibility that this electron in the conduction band and the electron-hole in valance band may recombine and decrease the efficiency of the process, but some of them which do not recombine, reach on the top of the surface as photo exited electrons and reduce the atmospheric oxygen or the hydroxyl radicals. The valance band hole may oxidize the surface absorbed water. The resulting reactive Oxygen species will further decompose the organic dirt into carbon dioxide and water, present on the surface. [57,58]

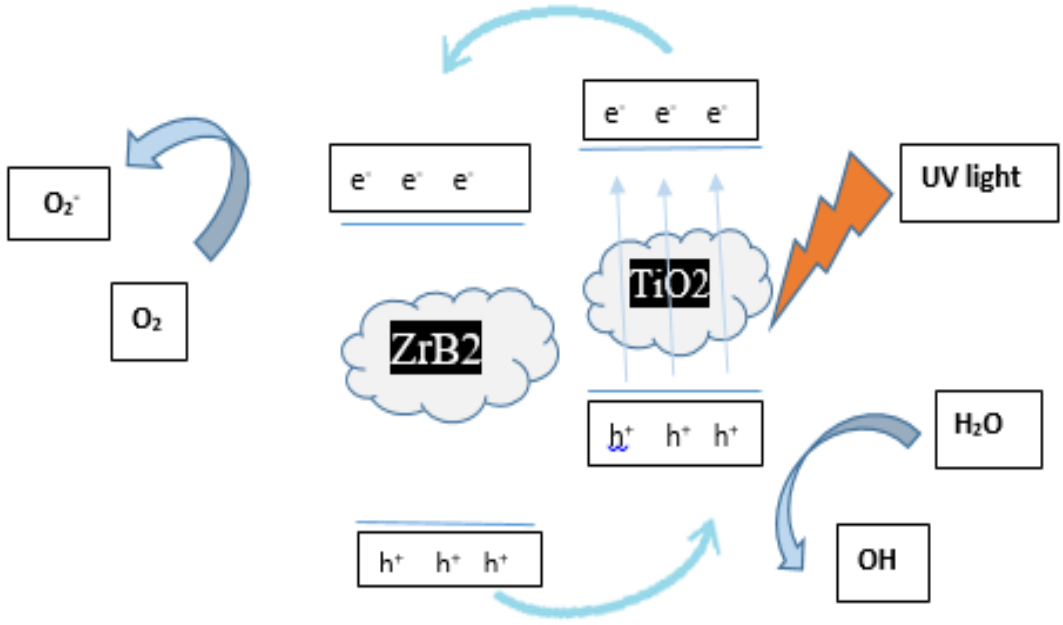

Fig. 4.10 schematic representation of photo degradation by ZrB_2 /TiO_2 nano composites

Following reactions will happen during photo degradation process,

$$TiO_2 – ZrB_2 + hv \rightarrow [TiO_2 - ZrB_2 (e–)]^*$$

$$[TiO_2 - ZrB_2 (e–)]^* + O_2 \rightarrow [TiO_2 - ZrB_2{}^{+}] + O_2{}^{--},$$

$O_2^{\cdot-}$ + organic compounds/dye (RhB) → degradation products.

These photo degradation reactions generally follow first order reaction kinetics [53] which is given by:

$$r = dC/dt = kKc/1+KC$$

Simplified as: $\ln C/C_0 = kKt = kt$.

where, k is first order rate constant.

The maximum efficiency of 85 % was achieved by the sample with 1% of ZrB_2 nanosheets. The catalyst with 0.5% and 2% of ZrB_2 nanosheets have shown 76% and 71 % maximum degradation efficiency in 60 minutes as shown in Fig. 4.6 (c).

Conclusion

ZrB_2 nanosheets were successfully synthesized by liquid phase exfoliation. Exfoliated nanosheets were then characterized by XRD,SEM, UV-Vis and AFM. Exfoliation of ZrB_2 into nanosheets was confirmed by the characterization techniques. New peaks observed in the XRD analysis confirmed the formation of ZrB_2 nanosheets. SEM and AFM analysis showed the average thickness of sheets to be less than 11nm and length approximately 1 micrometer. The UV-Visible graph showed the absorbance of nanosheets in UV region, recommended these sheets as UV-photoactive material. For photocatalytic activity ZrB_2 nanosheets were combined with commercial TiO_2 nanoparticles to prepare a photocatalyst material.

ZrB_2 /TiO_2 nanocomposites were prepared by ex situ addition of exfoliated ZrB_2 nanosheets at different weight ratios to study photocatalytic degradation of Rhodamine B under UV light. The photodegaradation efficiency of prepared samples increase from 0.5% to 1% ZrB_2 /TiO_2 nanocomposites with about 85% photo degradation of RhB in just 60 min.With further addition of nanosheets, the photodegradation efficiency decreases for 2% nano composites. The decrease in photodegradation efficiency is speculated to be due to agglomeration of nanosheets and fast recombination rate of charge carriers. From this research work it can be concluded that ZrB_2 itself is a good photocatalyst.

Future Recommendation

The prepared nanosheets have low thickness and 650nm lateral dimension which shows they have high aspect ratio and characterized by XRD, SEM, AFM and UV-Vis spectroscopy. The samples prepared were tested under UV light for photocatalysis.

In future these samples can be tested under visible irradiation by sensitizing ZrB_2 with some visible light absorbing material like MoS_2, PbS QDs and their effects could be studied. And also can be tested in energy storage. It can be further applicable for EMI shielding.

Zirconium diboride possesses properties like hardness, chemical inertness, oxidation resistance and high conductivity both thermally and electrically. The ZrB_2 nanosheets we can extend these advantages to nanoscale devices and products, for instance, electrodes, aircraft materials, durable electronics, and heterostructures incorporating other nanomaterials.

References:

[1] K. Miyazaki and N. I. Ã, “Nanotechnology systems of innovation — an analysis of industry and academia research activities,” vol. 27, pp. 661–675, (2007).

[2] V. Sundström, “Solar energy conversion.,” Dalton Trans., no. 45, p. 9951, (2009).

[3] S. T. Glassmeyer, E. T. Furlong, D. W. Kolpin, A. L. Batt, R. Benson, J. S. Boone, O. Conerly, M. J. Donohue, D. N. King, M. S. Kostich, H. E. Mash, S. L. Pfaller, K. M. Schenck, J. E. Simmons, E. A. Varughese, S. J. Vesper, E. N. Villegas, and V. S. Wilson, “Nationwide reconnaissance of contaminants of emerging concern in source and treated drinking waters of the United States,” Sci. Total Environ., vol. 581–582, pp. 909–922, (2017).

[4] S. Liu et al., “Enhanced Photocatalytic Degradation of Environmental Pollutants under Visible Irradiation by a Composite Coating,” Environ. Sci. Technol., vol. 51, no. 9, pp. 5137–5145, (2017), doi: 10.1021/acs.est.7b00350.

[5] P. Mazierski, A. Mikolajczyk, B. Bajorowicz, A. Malankowska, A. Zaleska-Medynska, and J. Nadolna, “The role of lanthanides in TiO2-based photocatalysis: A review,” Appl. Catal. B Environ., vol. 233, pp. 301–317, (2018), doi: 10.1016/j.apcatb.2018.04.019

[6] K. S. Novoselov, A. K. Geim, S. V. Morozov, D. Jiang, Y. Zhang, S. V. Dubonos, I. V. Grigorieva, and A. A. Firsov,Science 306, 666 (2004).

[7] Li, Jun. *Two-dimensional Materials: Growth, Characterization, and Simulation*. Diss. Carnegie Mellon University, (1918).

[8] Yousaf, Ahmed. *Liquid-phase Exfoliation and Applications of Pristine Two-dimensional Transition Metal Dichalcogenides and Metal Diborides*. Arizona State University, (2018).

[9] Mayrhofer, P. H., Kirnbauer, A., Ertelthaler, P., & Koller, C. M. (2018). High-entropy ceramic thin films; A case study on transition metal diborides. *Scripta Materialia, 149*, 93-97.

[10] W.G. Fahrenholtz, E.J. Wuchina, W.E. Lee, Y. Zhou (Eds.) (2014). Ultra-High Temperature Ceramics: Materials for Extreme Environment Applications, Wiley, New York

[11]Nicolosi, V., Chhowalla, M., Kanatzidis, M. G., Strano, M. S. & Coleman, J. N. Liquid Exfoliation of Layered Materials Liquid Exfoliation of Layered Materials. Science. 340, (2013).

[12] Wagner, F. R., Baranov, A. I., Grin, Y. & Kohout, M. A Position-Space View on Chemical Bonding in Metal Diborides with AlB_2 Type of Crystal Structure. Zeitschrift für Anorg. und Allg. Chemie 639, 2025–2035 (2013).

[13] Buzea, C. & Yamashita, T. Review of the superconducting properties of MgB_2. Supercond. Sci. Technol. 14, R115 (2001).

[14] Munro, R. G. Material Properties of Titanium Diboride. J. Res. Natl. Inst. Stand. Technol. 105, 709–720 (2000).

[15] Fahrenholtz, W. G., Hilmas, G. E., Talmy, I. G. & Zaykoski, J. A. Refractory diborides of zirconium and hafnium. J. Am. Ceram. Soc. 90, 1347–1364 (2007).

[16] Gu, Q., Krauss, G. & Steurer, W. Transition metal borides: Superhard versus ultraincompressible. Adv. Mater. 20, 3620–3626 (2008).

[17] Šimůnek, A. Anisotropy of hardness from first principles: The cases of ReB_2 and 91 OsB_2. Phys. Rev. B - Condens. Matter Mater. Phys. 80, 1–4 (2009).

[18] Mayrhofer, Paul H., et al. "High-entropy ceramic thin films; A case study on transition metal diborides." *Scripta Materialia* 149 (2018): 93-97.

[19] Tang, S., Deng, J., Wang, S., Liu, W., & Yang, K.” Ablation behaviors of ultra-high temperature ceramic composites”. *Materials Science and Engineering: A*, *465*(2007), 1-7.

[20] Fahrenholtz, W. G., & Hilmas, G. E. (2012). Oxidation of ultra-high temperature transition metal diboride ceramics. *International Materials Reviews*, *57*(1), 61-72.

[21] W.-R. Kim, H. Park, and W.-Y. Choi, "TiO_2 micro-flowers composed of nanotubes and their application to dye-sensitized solar cells.," Nanoscale Res. Lett., vol. 9, no. 1, p. 93, (2014).

[22] Y. Tang, P. Wee, Y. Lai, X. Wang, D. Gong, P. D. Kanhere, T. T. Lim, Z. Dong, and Z. Chen, "Hierarchical TiO_2 nanoflakes and nanoparticles hybrid structure for improved photocatalytic activity," J. Phys. Chem. C, vol. 116, no. 4, pp. 2772–2780, (2012).

[23] A. Fujishima and K. Honda, "TiO_2 photoelectrochemistry and photocatalysis," Nature, vol. 213, no. 1998, p. 8656, (1972).

[24] Y. Yang, J. X. Hu, Y. Liang, J. P. Zou, K. Xu, R. J. Hu, Z. D. Zou, Q. Yuan, Q. Q. Chen, Y. Lu, T. Yu, and C. L. Yuan, "Anatase TiO_2 hierarchical microspheres consisting of truncated nanothorns and their structurally enhanced gas sensing performance," J. Alloys Compd., vol. 694, pp. 292–299, (2017).

[25] O. Carp, C. L. Huisman, and A. Reller, "Photoinduced reactivity of titanium dioxide," Prog. Solid State Chem., vol. 32, no. 1–2, pp. 33–177, (2004).

[26] U. Diebold, "Structure and properties of TiO_2 surfaces: A brief review," Appl. Phys. A Mater. Sci. Process., vol. 76, no. 5, pp. 681–687, (2003).

[27] Qing GUO, Chuan-Yao ZHOU, Zhi-Bo MA, Ze-Feng REN, Hong-Jun FAN,Xue-Ming YANG, F. A. N. Hong-jun, "Fundamental Processes in Surface Photocatalysis on TiO2" Acta Phys. -Chim. Sin vol. 32, no. 1, pp. 28–47, (2016).

[28] J. Domaradzki, "Photocatalytic properties of Ti – V oxides thin films," Opt. Appl., vol. XLIII, no. 1, pp. 153–162, (2013).

[29]K. Hashimoto, H. Irie, and A. Fujishima, "A Historical Overview and Future Prospects," AAPPS Bull., vol. 17, no. 6, pp. 12–28, (2007).

[30] W.-R. Kim, H. Park, and W.-Y. Choi, "TiO_2 micro-flowers composed of nanotubes and their application to dye-sensitized solar cells," Nanoscale Res. Lett., vol. 9, no. 1, p. 93, (2014).

[31] K. L. Yeung, S. T. Yau, A. J. Maira, J. M. Coronado, J. Soria, and P. L. Yue, "The influence of surface properties on the photocatalytic activity of nanostructured TiO_2," J. Catal., vol. 219, no. 1, pp. 107–116, (2003).

[32] B. Ohtani, D. Li, and R. Abe, “What is Degussa (Evonik) P25 Crystalline composition analysis , reconstruction from isolate pure particles and ...,” no. October 2014, (2010).

[33] Z. Ren, Y. Guo, C.-H. Liu, and P.-X. Gao, “Hierarchically nanostructured materials for sustainable environmental applications.,” Front. Chem., vol. 1, no. November, p. 18, (2013).

[34] Z. Zheng, B. Huang, X. Qin, X. Zhang, and Y. Dai, “Strategic synthesis of hierarchical TiO_2 microspheres with enhanced photocatalytic activity,” Chem. - A Eur. J., vol. 16, no. 37, pp. 11266–11270, (2010).

[35] S. Eigler et al., "Wet chemical synthesis of graphene," vol. 25, no. 26, pp. 3583-3587, (2013).

[36] Y. Zhang, K. Fugane, T. Mori, L. Niu, and J. J. J. o. M. C. Ye, "Wet chemical synthesis of nitrogen-doped graphene towards oxygen reduction electrocatalysts without high-temperature pyrolysis," vol. 22, no. 14, pp. 6575-6580, (2012).

[37] P. Xiao, M. Xiao, and K. J. P. Gong, "Preparation of exfoliated graphite/polystyrene composite by polymerization-filling technique," vol. 42, no. 11, pp. 4813-4816, (2001).

[38] W. Feng, P. Long, Y. Feng, and Y. J. A. S. Li, "Two- dimensional fluorinated graphene: synthesis, structures, properties and applications," vol. 3, no. 7, p. 1500413, (2016).

[39] A. Ciesielski and P. J. C. S. R. Samorì, "Graphene via sonication assisted liquid-phase exfoliation," vol. 43, no. 1, pp. 381-398, (2014).

[40] J. N. J. A. F. M. Coleman, "Liquid- phase exfoliation of nanotubes and graphene," vol. 19, no. 23, pp. 3680-3695, (2009).

[41] A. B. Bourlinos, V. Georgakilas, R. Zboril, T. A. Steriotis, and A. K. J. s. Stubos, "Liquid- phase exfoliation of graphite towards solubilized graphenes," vol. 5, no. 16, pp. 1841-1845, (2009).

[42] T. Matsunaga, R. Tomoda, T. Nakajima, and H. Wake, “Photoelectrochemical sterilization of microbial cells by semiconductor powders,” FEMS Microbiol. Lett., vol. 29, no. 1, pp. 211–214, (1985).

[43] M. Janus, A. Markowska-Szczupak, E. Kusiak-Nejman, and A. W. Morawski, "Disinfection of E. coli by carbon modified TiO_2 photocatalysts," Environ. Prot. Eng., vol. 38, no. 2, pp. 89–97, (2012).

[44] AFM, A. F. M. Basic Theory.

[45] Marrese, M., Guarino, V., & Ambrosio, L. (2017). Atomic force microscopy: a powerful tool to address scaffold design in tissue engineering. *Journal of functional biomaterials*, *8*(1), 7.

[46] M. Naderi, "Surface Area," in Progress in Filtration and Separation, Elsevier, pp. 585–608, (2015).

[47] Zhang, G. J., Deng, Z. Y., Kondo, N., Yang, J. F., & Ohji, T. (2000). Reactive hot pressing of ZrB_2–SiC composites. *Journal of the American Ceramic Society*, *83*(9), 2330-2332.

[48] An, Y., Xu, X., & Gui, K. (2016). Effect of SiC whiskers and graphene nanosheets on the mechanical properties of ZrB_2-SiCw-Graphene ceramic composites. *Ceramics International*, *42*(12), 14066-14070.

[49] Zhang, Y., Li, R., Jiang, Y., Zhao, B., Duan, H., Li, J., & Feng, Z. (2011). Morphology evolution of ZrB_2 nanoparticles synthesized by sol–gel method. *Journal of Solid State Chemistry*, *184*(8), 2047-2052.

[50] Wang, L., Zhao, D., Cheng, Q., Lu, Q., Liu, W., Bao, K. & Zhou, Q. (2018). Iodine-assisted solid-state synthesis and characterization of nanocrystalline zirconium diboride nanosheets. *Journal of Superhard Materials*, *40*(4), 254-258.

[51] An, Y., Han, J., Han, W., Zhao, G., Xu, B., Jin, K., & Zhang, X. (2016). Chemical vapor deposition synthesis carbon nanosheet–coated zirconium diboride particles for improved fracture toughness. *Journal of the American Ceramic Society*, *99*(4), 1360-1366.

[52] Khan, R., Riaz, A., Javed, S., Jan, R., Akram, M. A., & Mujahid, M. (2018). Synthesis and characterization of MoS_2/TiO_2 nanocomposites for enhanced photocatalytic degradation of methylene blue under sunlight irradiation. In *Key Engineering Materials* (Vol. 778, pp. 137-143). Trans Tech Publications Ltd.

[53] Khan, R., Riaz, A., Rabeel, M., Javed, S., Jan, R., & Akram, M. A. (2019). TiO_2@$NbSe_2$ decorated nanocomposites for efficient visible-light photocatalysis. *Applied Nanoscience*, *9*(8), 1915-1924.

[54] Patidar, R., Gunda, H., Varma, A. K., Gawas, R., Das, S. K., & Jasuja, K. (2020). Co-solvent exfoliation of layered titanium diboride into few-layer-thick nanosheets. *Ceramics International*, *46*(18), 28324-28331.

[55] Zhu, L., Zhao, X., Li, Y., Yu, X., Li, C., & Zhang, Q. (2013). High-quality production of graphene by liquid-phase exfoliation of expanded graphite. *Materials Chemistry and Physics*, *137*(3), 984-990.

[56] Wei, X., Zhu, G., Fang, J., & Chen, J. (2013). Synthesis, characterization, and photocatalysis of well-dispersible phase-pure anatase TiO_2 nanoparticles. *International Journal of Photoenergy*, *2013*.

[57] Jie, Z., Xiao, X., Huan, Y., Youkang, H., & Zhiyao, Z. (2021). The preparation and characterization of TiO_2/r-GO/Ag nanocomposites and its photocatalytic activity in formaldehyde degradation. *Environmental technology*, *42*(2), 193-205.

[58] Xiao, F. X., Miao, J., & Liu, B. (2014). Layer-by-layer self-assembly of CdS quantum dots/graphene nanosheets hybrid films for photoelectrochemical and photocatalytic applications. *Journal of the American Chemical Society*, *136*(4), 1559-1569.

[59] Alamelu, K., Raja, V., Shiamala, L., & Ali, B. J. (2018). Biphasic TiO_2 nanoparticles decorated graphene nanosheets for visible light driven photocatalytic degradation of organic dyes. *Applied Surface Science*, *430*, 145-154.

[60] Saravanan, R., Gracia, F., & Stephen, A. (2017). Basic principles, mechanism, and challenges of photocatalysis. In *Nanocomposites for visible light-induced photocatalysis* (pp. 19-40). Springer, Cham.

[61]Geim, A. K., & Grigorieva, I. V. (2013). Van der Waals heterostructures. *Nature*, *499*(7459), 419-425.

[62] Sunko, V., Milosavljević, D., Mazzola, F., Clark, O. J., Burkhardt, U., Kim, T. K. & King, P. D. C. (2020). Surface and bulk electronic structure of aluminium diboride. *Physical Review B*, *102*(3), 035143.

[63] Li, H., Zhang, L., Zeng, Q., Wang, J., Cheng, L., Ren, H., & Guan, K. (2010). Crystal structure and elastic properties of ZrB compared with ZrB_2: A first-principles study. *Computational Materials Science*, *49*(4), 814-819.

[64] Yi, M., & Shen, Z. (2015). A review on mechanical exfoliation for the scalable production of graphene. *Journal of Materials Chemistry A*, *3*(22), 11700-11715.

[65] Huo, C., Yan, Z., Song, X., & Zeng, H. (2015). 2D materials via liquid exfoliation: a review on fabrication and applications. *Science bulletin*, *60*(23), 1994-2008.